Geophysical Research Letters

RESEARCH LETTER
10.1029/2020GL089429

Special Section:
Fire in the Earth System

Summer $PM_{2.5}$ Pollution Extremes Caused by Wildfires Over the Western United States During 2017–2018

Yuanyu Xie[1,2], Meiyun Lin[1,2], and Larry W. Horowitz[2]

[1]Atmospheric and Oceanic Sciences, Princeton University, Princeton, NJ, USA, [2]NOAA Geophysical Fluid Dynamics Laboratory, Princeton, NJ, USA

Key Points:
- Large interannual variations of western U.S. fine particulate pollution in summer were driven by regional and distant fires
- Widespread wildfires and stagnation in 2017–2018 caused fine particulate extremes to exceed 2 standard deviations over long-term averages
- Observations and model analyses indicate fourfold to fivefold underestimate of aerosol emissions from the widely used Global Fire Emissions Database

Supporting Information:
- Supporting Information S1

Correspondence to:
Y. Xie,
yuanyu.xie@noaa.gov

Citation:
Xie, Y., Lin, M., & Horowitz, L. W. (2020). Summer $PM_{2.5}$ pollution extremes caused by wildfires over the western United States during 2017–2018. *Geophysical Research Letters*, *47*, e2020GL089429. https://doi.org/10.1029/2020GL089429

Received 24 JUN 2020
Accepted 22 JUL 2020
Accepted article online 29 JUL 2020

Abstract Using observations and model simulations (ESM4.1) during 1988–2018, we show large year-to-year variability in western U.S. $PM_{2.5}$ pollution caused by regional and distant fires. Widespread wildfires, combined with stagnation, caused summer $PM_{2.5}$ pollution in 2017 and 2018 to exceed 2 standard deviations over long-term averages. ESM4.1 with a fire emission inventory constrained by satellite-derived fire radiative energy and aerosol optical depth captures the observed surface $PM_{2.5}$ means and extremes above the 35 $\mu g/m^3$ U.S. air quality standard. However, aerosol emissions from the widely used Global Fire Emissions Database (GFED) must be increased by 5 times for ESM4.1 to match observations. On days when observed $PM_{2.5}$ reached 35–175 $\mu g/m^3$, wildfire emissions can explain 90% of total $PM_{2.5}$, with smoke transported from Canada contributing 25–50% in northern states, according to model sensitivity simulations. Fire emission uncertainties pose challenges to accurately assessing the impacts of fire smoke on air quality, radiation, and climate.

Plain Language Summary Frequent and intense wildfires harm public health over the western United States. In order to understand how wildfires affect fine particulate air quality, we analyze surface and satellite measurements and computer model simulations of weather and atmospheric chemistry over the past 30 years. We show that widespread fires and regional transport of fire smoke are the main causes of year-to-year changes in summertime particle pollution measured at western U.S. surface sites. The U.S. Environmental Protection Agency defines daily particle concentration above 35 $\mu g/m^3$ as unhealthy. In the summers of 2017–2018, record-breaking wildfires, combined with stable weather conditions, resulted in daily particle concentration of 35 to 175 $\mu g/m^3$ across western U.S. sites. These particle pollution extremes are twice as severe as long-term average conditions. Wildfire emissions contributed 90% of particle levels on these periods. Notably, transport of fire smoke from southwestern Canada can explain 25% to 50% of particle pollution in northern states such as Washington. Our model successfully simulates these pollution extremes when applying a fire emission data set constrained by satellite observations of total particle abundances. Our results indicate fourfold to fivefold underestimates of particle emissions from the widely used Global Fire Emissions Database not constrained by satellite observations.

1. Introduction

Warmer springs and earlier snowmelt have resulted in severe drought and wildfires in the western United States (WUS) over recent decades (Abatzoglou & Williams, 2016; Westerling et al., 2006). A number of studies report a tight connection between wildfires and aerosol abundances over the WUS during summer (Hallar et al., 2017; Jaffe et al., 2008; Mallia et al., 2015; McClure & Jaffe, 2018; O'Dell et al., 2019), with implications for public health (e.g., Reid et al., 2016). Here we build on early work by systematically investigating the impacts of local, regional, and distant fires on fine particulate matter ($PM_{2.5}$) in WUS surface air and aerosol abundances aloft during 1988–2018, with a particular focus on the recent extremes of 2017 and 2018.

During the summers of 2017–2018, severe drought and heatwaves scorched western North America (Hoell et al., 2019; LeComte, 2019; H. Wang et al., 2019), providing favorable conditions for burning of biomass accumulated in the preceding wet spring (Balch et al., 2018). Over 3.5×10^6 ha was burned across the United States in 2017 and 2018, 45% larger than the average over the past two decades (NICC, 2019). In southwestern Canada, wildfires set records for the longest Provincial State of Emergency (70 days) in 2017 and for the greatest area burned ($>1.3 \times 10^6$ ha) in 2018 (GBC, 2019). Some WUS cities experienced peak $PM_{2.5}$ concentrations of 100–642 $\mu g/m^3$ during intense burning periods (Laing & Jaffe, 2019).

The 2017–2018 extremes provide a rare opportunity to evaluate chemistry-climate models needed to assess the impacts of wildfires in a warming climate. However, fire emissions used in these models are highly uncertain: Organic carbon emissions in six datasets differ by a factor of 10 over North America (Carter et al., 2020; Pan et al., 2020). Uncertainties also exist in the vertical distribution of fire smoke (Paugam et al., 2016; Rémy et al., 2017; Zhu et al., 2018) and in the representation of fire plume chemistry (Posner et al., 2019; Shrivastava et al., 2015). Using the Geophysical Fluid Dynamic Laboratory Earth System Model (GFDL ESM4.1; Horowitz et al., 2020), we conduct a suite of decadal simulations (2003–2018) designed to isolate the impacts of fire emission source strength, injection height, and local and Canadian fires on surface $PM_{2.5}$ extremes over the WUS.

2. Methods

2.1. Observations

We use surface observations of $PM_{2.5}$ and its speciation from the Interagency Monitoring of Protected Visual Environments (IMPROVE) network (predominantly in rural locations) during 1988–2018. Data are available for every 3 days. To provide constraints on simulated aerosol abundance aloft, we incorporate aerosol optical depth (AOD) from the MODerate resolution Imaging Spectroradiometer (MODIS; merged Dark Target and Deep Blue products, Collection 6.1, Level 3 at $1° \times 1°$ resolution) for 2000–2018 (Remer et al., 2005; Sayer et al., 2014) and aerosol extinction profiles from the Cloud-Aerosol Lidar with Orthogonal Polarization instrument (CALIOP; Level 2, Version 4-20) for 2017–2018 (Watson-Parris et al., 2018; Winker et al., 2013). Details of satellite data processing are provided in supporting information Text S1. Meteorological conditions affecting particulate matter (PM) extremes during 2017–2018 are analyzed, including the severity of drought conditions represented by the Standardized Precipitation Evapotranspiration Index (Vicente-Serrano et al., 2010) and air stagnation index (ASI) from the U.S. National Climatic Data Center (Wang & Angell, 1999; Text S2).

2.2. Models

We use the GFDL ESM4.1 global model with interactive stratosphere-troposphere chemistry at a horizontal resolution of ~100×100 km^2 (Horowitz et al., 2020). The model is nudged to NCEP (National Center for Environmental Prediction) horizontal winds using a pressure-dependent nudging technique (Lin et al., 2012, 2015). Anthropogenic emissions are from the Coupled Model Intercomparison Project Phase 6 (CMIP6) (Hoesly et al., 2018). Biogenic isoprene and terpene emissions are tied to model meteorology (Guenther et al., 2012). We make several modifications from the default model settings, in particular reverting the coupled dust emission scheme (Evans et al., 2016) to that used in AM4.0 (Zhao et al., 2018) and lowering the secondary organic aerosol (SOA) yield from isoprene and terpenes from 10% to 4% (Heald et al., 2006; Veefkind et al., 2011), to improve $PM_{2.5}$ simulations over North America (see Figures S1–S3 and Text S3).

The standard version of ESM4.1 uses monthly fire emissions from CMIP6 and simplified vertical distributions across the major latitude zones following Dentener et al. (2006). Here we implement daily fire emissions from the Global Fire Emissions Database (GFED4.1s) (Randerson et al., 2012; van der Werf et al., 2017) and from the Quick Fire Emissions Dataset (QFED v2.5) (Darmenov & da Silva, 2015). For both datasets, we apply monthly gridded fire injection heights observed by the Multiangle Imaging Spectro Radiometer (MISR) (Val Martin et al., 2018), with 15–50% of fire emissions across North America injected above the boundary layer (Figure S4). QFED, with fire emissions based on satellite observations of fire radiative power and constrained by MODIS AOD (Darmenov & da Silva, 2015), produces 3 to 5 times higher black carbon (BC) and organic carbon (OC) emissions than GFED over North America (Figures S5 and S6). With these changes, we conduct a suite of hindcast simulations for 2003–2018 to investigate the relationship between fires and aerosol abundances (Table S1).

2.3. Analysis Method

We examine the impacts of fires on the observed and simulated means and the 95th percentile (q95) of June–September (JJAS) daily $PM_{2.5}$ concentrations across all WUS sites (~2,500 samples per summer) as well as the maximum and BC and OC of daily $PM_{2.5}$ at individual sites. Models are sampled on days and locations where observations are available. Considering substantial uncertainties in aerosol emissions from

different inventories, we use total carbon emissions (including CO_2, CO, and CH_4) from GFED4.1s to represent the severity of fires for the regression analysis (section 3.1). To assess the impact from local versus distant fires on $PM_{2.5}$ at each site, we vary the size of the box within which fire emissions of carbon are integrated, from 0.5° × 0.5° to 20° × 20° centered at that site (Text S4 and Figure S7). Detailed analytical methods are given alongside the results in section 3.

3. Results

3.1. Observed Interannual Correlations Between $PM_{2.5}$ and Wildfires

We first examine the extent to which surface $PM_{2.5}$ measured at IMPROVE sites is correlated with local and remote fires on interannual time scales. Figure 1a shows the correlations (r^2) of the observed JJAS mean $PM_{2.5}$ at each site with the JJAS total carbon emissions from fires integrated over a box where the maximum correlation is found. Most WUS sites show the highest correlation (r^2 = 0.6–0.8) with fire emissions integrated over a box of 10° × 10° to 15° × 15°, indicating the importance of regional smoke transport. Interannual variability of the q95 $PM_{2.5}$ at each site is best correlated with fires burned in a region greater than 1,000 × 1,000 km^2 around that site (Figure S8).

Figure 1b further stresses the strong relationship of WUS $PM_{2.5}$ extremes with regional fire emissions, showing yearly time series of JJAS total fire emissions of carbon in the WUS and southwestern Canada, along with yearly time series of JJAS q95 $PM_{2.5}$ across all WUS sites. Higher correlation is found when fire emissions are summed over the WUS and southwestern Canada (r^2 = 0.74) compared to when only WUS emissions are considered (r^2 = 0.55), indicating the importance of cross-boundary transport. The strong fire-$PM_{2.5}$ relationship is supported by the correlation with organic aerosol (OA, r^2 = 0.80), a key component of $PM_{2.5}$ in fire smoke. The ratio of OA to $PM_{2.5}$ increases from <0.5 in the early 1990s to >0.8 in the recent decade, resulting from the coincident increases in wildfire emissions and reductions in anthropogenic emissions. The JJAS q95 $PM_{2.5}$ and OA over the WUS during 2017–2018 exceeded the 1988–2016 averages by over 2 standard deviations.

Wildfires contribute to the observed increases in q95 $PM_{2.5}$ and OA over the WUS during summer (Figure 1c). The trends reported here are higher than those in McClure and Jaffe (2018), which did not include the 2017–2018 extremes. In contrast to WUS sites, decreasing $PM_{2.5}$ trends are recorded at eastern United States (EUS) sites over this period, driven by reduced anthropogenic sulfate. Increasing wildfires have largely offset efforts of regional emission controls that would otherwise have led to improved air quality over the WUS (Hand et al., 2012; McClure & Jaffe, 2018; Paulot et al., 2017).

3.2. $PM_{2.5}$ Extremes in the Summers of 2017–2018

Figure 2 examines anomalies in $PM_{2.5}$ extremes, fires, and associated meteorological conditions in 2017–2018. The q95 $PM_{2.5}$ concentrations doubled at 40% of the WUS sites during 2017 and 2018, compared to long-term conditions (Figures 2a and 2d). In 2017, 14% of the WUS sites (12% in 2018) have the annual 98th percentile of $PM_{2.5}$ exceeding the 35 $\mu g/m^3$ U.S. air quality standard, compared to less than 2% for low-fire years. Intense fires burned in northern California, Oregon, Montana, and British Columba in Canada under severe drought conditions, as illustrated with the Standardized Precipitation and Evapotranspiration Index (Figures 2b–2c and 2e–2f).

Anomalous northerly winds facilitated smoke transport from Canada into the WUS. Including fire emissions from southwestern Canada improves the fire-$PM_{2.5}$ correlations (comparing Figures 2g and 2h). Nonetheless, there remain deviations in the 2017–2018 $PM_{2.5}$ levels that are not fully explained by fire emissions. In August 2017 and 2018, when fires peak seasonally, more than half of the area in the WUS experienced greater than 1 standard deviation over long-term average stagnation days (Figures 2c and 2f). To account for both the influences from emissions and stagnation, we develop a stagnation-weighted fire impact index (Fire_ASI):

$$\text{Fire\_ASI}_i = (\text{Fire\_WUS}_i + \text{Fire\_Canada}_i) \times (\text{ASI\_WUS}_i / \text{ASI\_WUS}_{\text{mean}})$$

where i represents year; Fire_WUS_i and Fire_Canada_i represent total fire emissions of carbon over the WUS and southwestern Canada, respectively; ASI_WUS_i is the ASI averaged over WUS grids for each

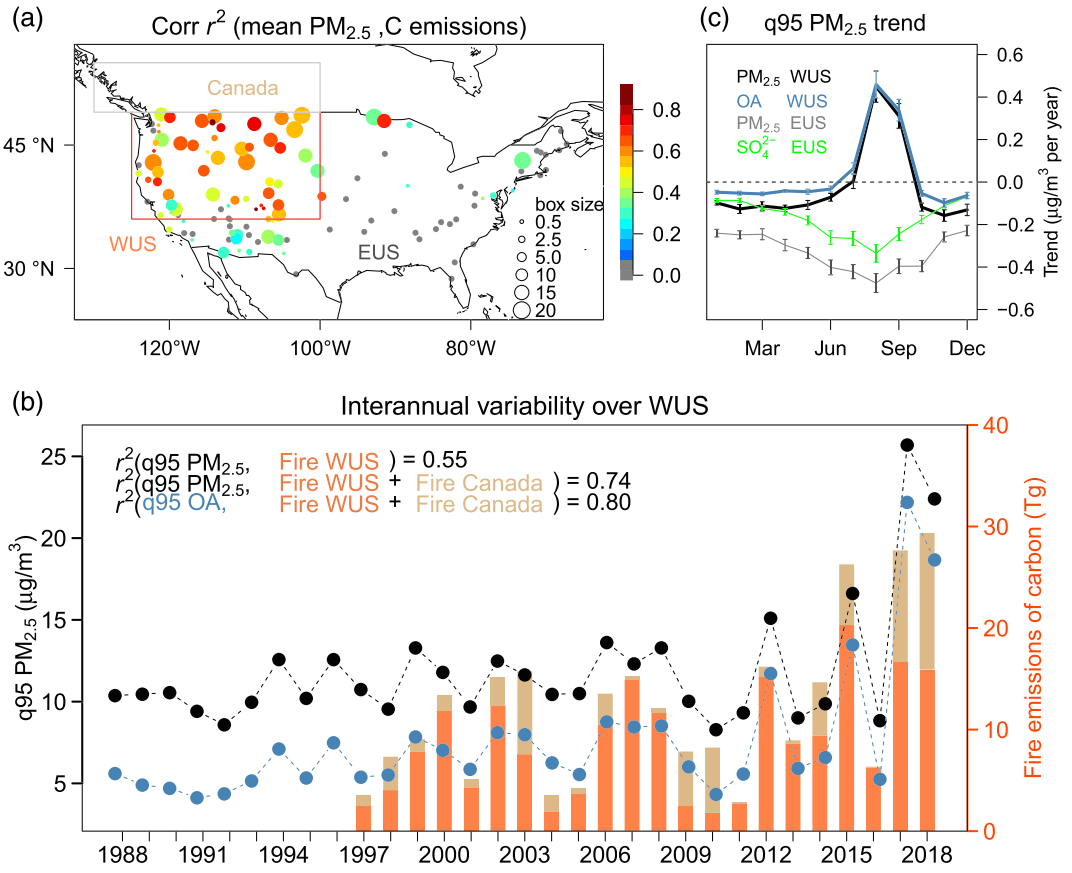

Figure 1. (a) Interannual correlations (r^2) between the June–September (JJAS) average $PM_{2.5}$ at individual IMPROVE sites and the JJAS total carbon emissions from fires integrated over a box (0.5° × 0.5° to 20° × 20°) surrounding each site during 1997–2018. The width of the box, within which the total fire emissions are best correlated with $PM_{2.5}$ at that site, is given in the right corner. Gray denotes sites with insignificant correlations ($p > 0.05$); (b) time series of the 95th percentile (q95) of JJAS daily $PM_{2.5}$ and organic aerosol (OA) concentrations across all WUS sites (red box in a), along with the JJAS total fire emissions of carbon over the WUS (orange) and southwestern Canada (brown, gray box in a). (c) The 1988–2018 trends of the q95 $PM_{2.5}$, OA, and sulfate for each month averaged over the WUS (red box) versus over the rest of the country (denoted as EUS); error bars represent standard error of the trends.

year, and ASI_WUS_{mean} is the 1997–2018 average. We use August ASI when fires and stagnation are most intense. Accounting for the influence from stagnation leads to an improved fire-$PM_{2.5}$ relationship ($r^2 = 0.87$ in Figure 2i vs. $r^2 = 0.74$ in Figure 2h), indicating that persistent stagnation exacerbated the buildup of $PM_{2.5}$ from fires during 2017–2018.

3.3. Model Simulation of Aerosols From Wildfires

We examine the capability of ESM4.1 in simulating the fire-aerosol relationship constrained by surface $PM_{2.5}$ observations, satellite-derived AOD, and aerosol extinction profiles (Figures 3 and S9–S11). ESM4.1 driven by GFED emissions (green lines in Figure 3; ESM4_GFED) substantially underestimates the observed $PM_{2.5}$ in surface air and satellite-derived AOD. The underestimates persist in both the mean values (Figures 3a and 3b) and the q95 (Figures 3c and 3d). During 2017–2018, the mean and q95 of $PM_{2.5}$ in ESM4_GFED are less than half of the observed values. We found little difference in AOD observed by MODIS Aqua, over an overpass time of 1:30 p.m., versus Terra, over an overpass time of 10:30 a.m. (black vs. gray symbols in Figures 3b and 3d), suggesting that the model-observation discrepancies are unlikely due to a lack of diurnal variations of fire emissions in our model. Supporting this statement, Mu et al. (2011) found small improvements in simulated carbon monoxide column when shifting fire emissions from daily to 3-hourly. The low-$PM_{2.5}$ bias over the WUS reflects underestimates in OA (Figure 3e), especially during

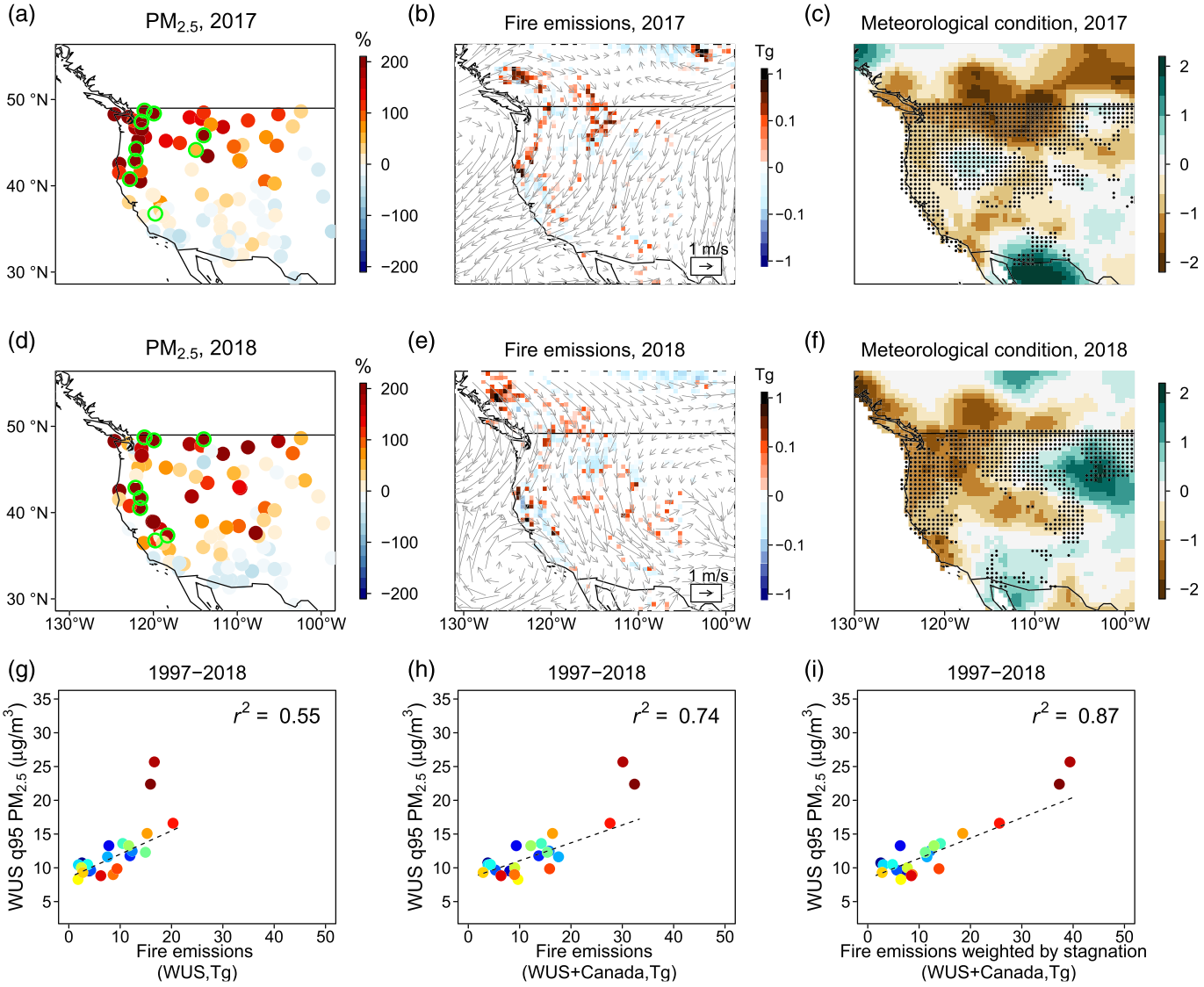

Figure 2. (a, d) Observed JJAS q95 $PM_{2.5}$ anomalies (in percentages relative to 2003–2016 q95 averages) for 2017 and 2018; green circles denote sites with the annual 98th percentile $PM_{2.5}$ exceeding 35 μg/m^3. (b, e) JJAS anomalies of total carbon emissions from fires and NCEP horizontal winds at 700 hPa. (c, f) Standardized precipitation evapotranspiration index for June–August 2017 and 2018; black stippling indicates grids where the August air stagnation index is 1 standard deviation greater than long-term averages. (g) Scatter plots of the q95 $PM_{2.5}$ (y axis) and total fire carbon emissions over the WUS (x axis). (h) Same as (g) but includes fire emissions from southwestern Canada. (i) Same as (h) but fire emissions are weighted by stagnation.

years with large fires (Figure S9), while the model captures OA concentrations over the EUS, where fire emissions are not the dominant contributor to $PM_{2.5}$ (Figure 3f).

Several studies using GFED emissions show that they were able to capture mean surface $PM_{2.5}$ observed at IMPROVE sites; however, they emit all fire emissions within the boundary layer (Carter et al., 2020; O'Dell et al., 2019; Spracklen et al., 2007). Our GFED_SFC simulation with fire emissions emitted in surface air also captures the observed surface $PM_{2.5}$ levels but still substantially underestimates satellite-derived AOD and aerosol extinction profiles (blue lines in Figures 3a–3d and S10). Besides, the interannual correlation of surface $PM_{2.5}$ with observations decreases: r^2 = (0.56, 0.65) in GFED_SFC, compared to r^2 = (0.79, 0.86) in ESM4_GFED with satellite-derived fire injection height. Other modeling studies using GFED also identified large underestimations of AOD over fire-prone regions (Pan et al., 2020; Petrenko et al., 2017; Reddington et al., 2016; Tosca et al., 2013). It is therefore critical to evaluate aerosol abundance both in surface air and aloft to ensure that models are right for the right reasons.

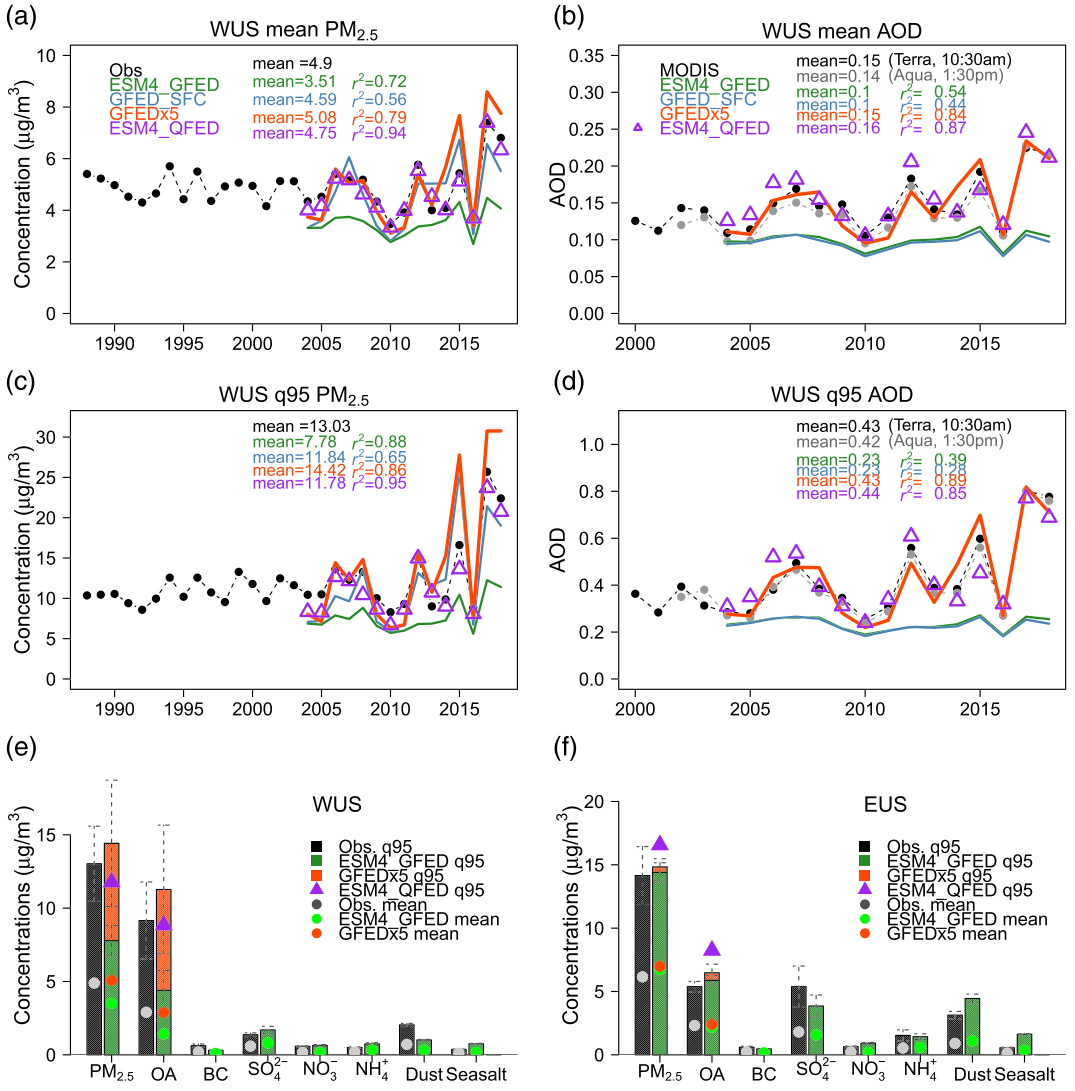

Figure 3. (a) Interannual variability of the WUS JJAS mean surface $PM_{2.5}$ during 1988–2018 from observations and ESM4.1 simulations sampled at observation sites and dates. ESM4_GFED = using GFED4.1s fire emissions and satellite-based injection height. GFED_SFC = with all fire emissions constrained at the surface. GFED×5 = with fire emissions increased by a factor of 5 but injection height as in ESM4_GFED. ESM4_QFED = using QFED fire emissions and satellite-based injection height. (b) Time series of JJAS mean AOD from MODIS Terra and Aqua observations and ESM4.1 simulations sampled at MODIS grids and dates; (c, d) same as (a, b) but for q95. (e, f) the 2003–2018 averages of the JJAS q95 (bars) and mean (circles) $PM_{2.5}$ and its major components for the WUS versus EUS sites.

We explore the influence from emission uncertainties with two sensitivity simulations: one with fire emissions from GFED increased by 5 times over the WUS and southwestern Canada (GFED×5) and the other using QFED emissions (ESM4_QFED). Satellite-based fire injection heights are applied in both experiments. OC emissions from QFED are approximately 5 times larger than those from the original GFED inventory over the WUS (Figure S6).

The GFED×5 experiment (red lines) substantially improves simulated aerosol abundances at the surface and aloft. Mean $PM_{2.5}$ over the WUS increase by 46% in ESM4.1 with GFED×5. The interannual correlation with observed mean AOD increases from $r^2 = 0.54$ in ESM4_GFED to $r^2 = 0.84$ in GFED×5. The GFED×5 simulation overestimates surface $PM_{2.5}$ during the high-fire years of 2015, 2017, and 2018. ESM4_QFED shows a higher correlation of $r^2 = (0.94,0.95)$ with observations, compared to $r^2 = (0.79, 0.86)$ in GFED×5. Increases

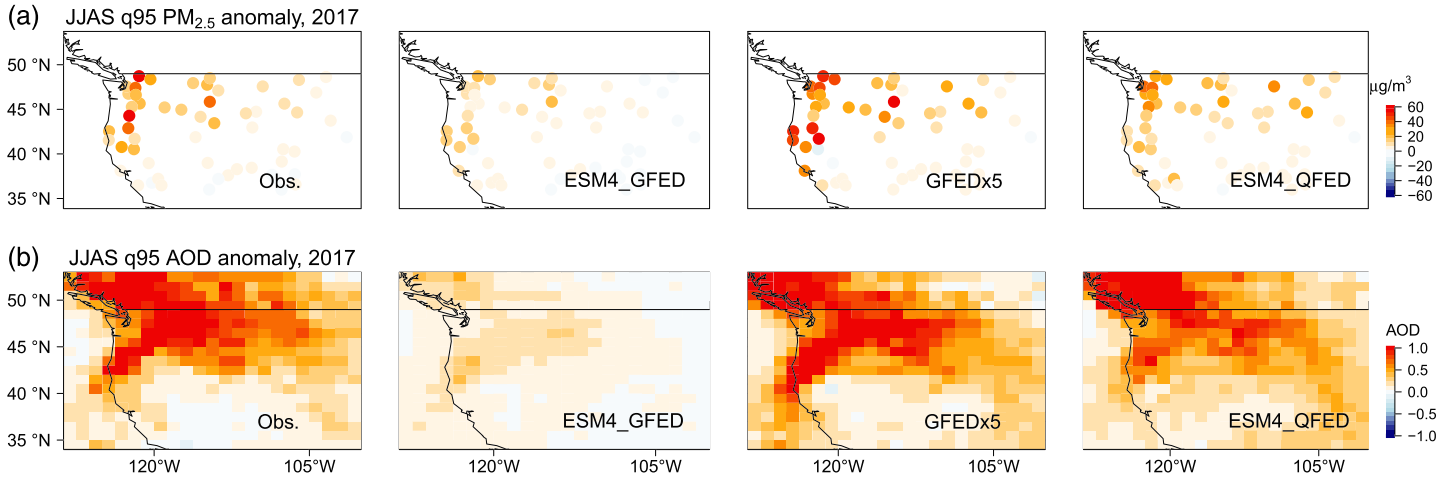

Figure 4. (a) The q95 surface $PM_{2.5}$ anomalies in JJAS 2017 (relative to 2003–2016 q95 averages) from observations and simulations with ESM4_GFED, with GFED×5 emissions and with ESM4_QFED; (b) same as the top panels but for AOD.

in surface $PM_{2.5}$ over the WUS in both GFED×5 and ESM4_QFED experiments primarily reflect increases in OA (Figure 3e).

Considering that $PM_{2.5}$ pollution associated with fires is highly heterogenous in space and time, we further examine the model's ability to simulate $PM_{2.5}$ extremes at individual IMPROVE sites during 2017–2018 (Figures 4 and S11). Observations show that anomalies in the q95 $PM_{2.5}$ during 2017 are 20–60 $\mu g/m^3$ at most IMPROVE sites. Both ESM4_QFED and GFED×5 simulations capture the observed anomalies, whereas the anomalies in ESM4_GFED are below 20 $\mu g/m^3$. Satellite observations show broad enhancements in AOD, extending from British Columbia in Canada to the U.S. Pacific northwestern states, consistent with ESM4_QFED and GFED×5 simulations.

We further evaluate simulated midtropospheric carbon monoxide (CO) with satellite observations (Figure S12). ESM4_GFED generally captures anomalies in mean 500 hPa CO during the peak fire months in 2017–2018, while CO anomalies in ESM4.1 with GFED×5 are a factor of 4 too high. This evaluation provides a hint that underestimates of aerosol emissions in GFED may be more specifically related to biases in the emission factors applied for aerosol species, instead of biases in satellite-based fire detection, simulation of biomass, or parameterization of fuel consumption. Recent field measurements reported that the OA emission factors for North American wildfires are 2 to 4 times greater than those commonly used in global fire emission inventories (e.g., Liu et al., 2017; Prichard et al., 2020).

We acknowledge that the simplified treatment of SOA in ESM4.1 may contribute to some of the model biases in aerosol abundances. Uncertainties in the chemical composition of OA may affect the calculation of hygroscopic growth and optical properties of aerosols in models. Several studies show that incorporating more detailed SOA chemistry improves simulated aerosol loadings in their models (Jathar et al., 2014; Posner et al., 2019; Shrivastava et al., 2015). However, a majority of field studies have reported little net OA formation during the fire plume transport and aging processes, as SOA accumulation is compensated by primary OA evaporation (Cubison et al., 2011; Garofalo et al., 2019; Jolleys et al., 2015; May et al., 2015; Selimovic et al., 2019; Shrivastava et al., 2017; Zhou et al., 2017).

3.4. Attribution of the 2017 and 2018 $PM_{2.5}$ Extremes

During the 2017 wildfire season, 50% of the WUS IMPROVE sites recorded maximum daily $PM_{2.5}$ above the 35 $\mu g/m^3$ U.S. air quality standard (Figure 5). Notably, 11% of the sites recorded concentrations above 100 $\mu g/m^3$, with severe impacts on air quality and visibility. Both ESM4 simulations with GFED×5 and QFED emissions capture the high-$PM_{2.5}$ events, although the GFED×5 simulation with higher emissions during 2017–2018 (Figure S6) better simulates some peak episodes. Stagnant, hot, and dry conditions during an active wildfire season may facilitate the buildup of pollution produced from regional or local anthropogenic emissions, complicating the unambiguous attribution of observed high ozone events to wildfire

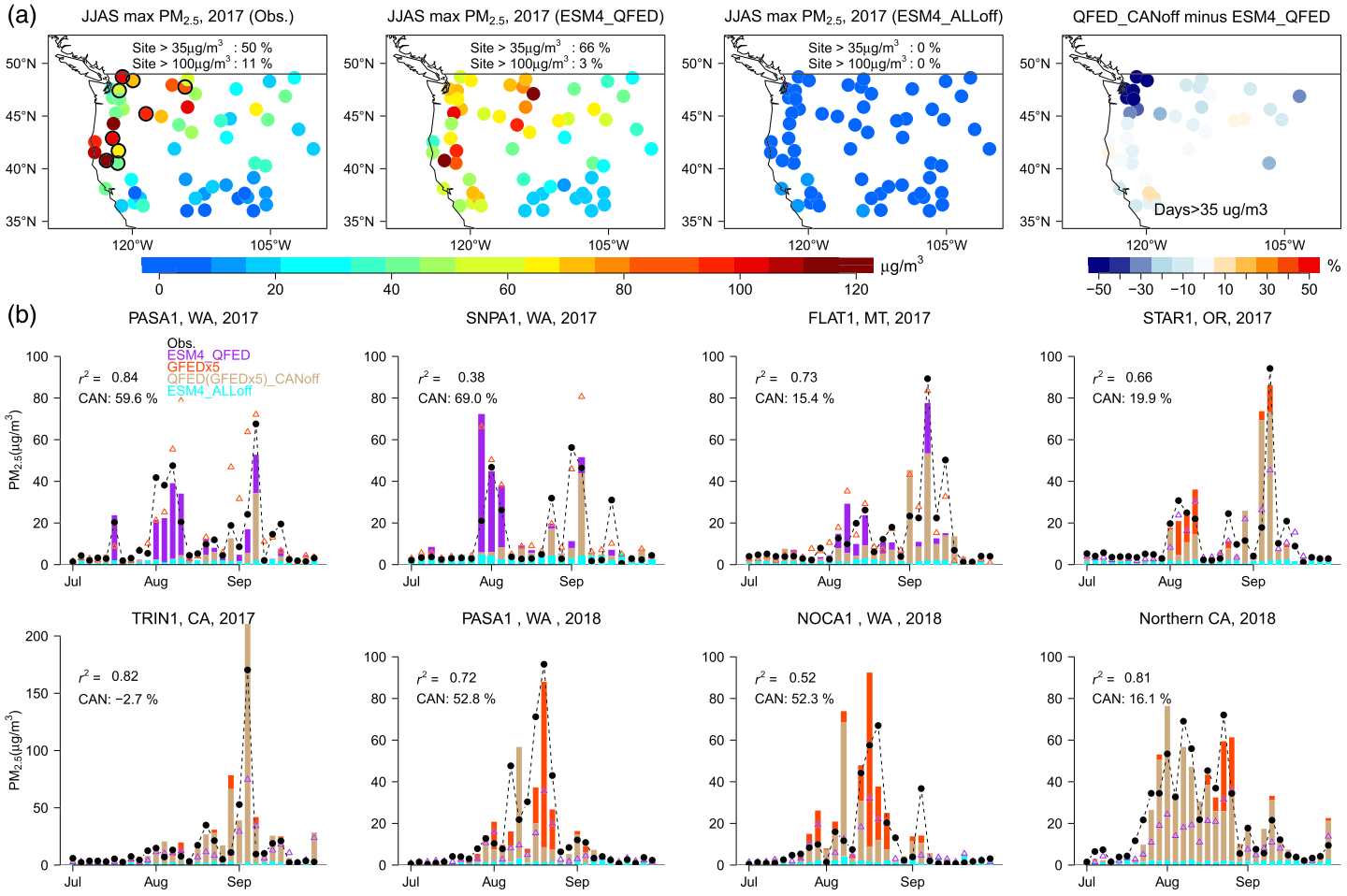

Figure 5. (a) The JJAS maximum $PM_{2.5}$ in 2017 from observations and ESM4.1 simulations, and the percentage contribution of Canadian fires on days when total $PM_{2.5}$ exceeds 35 μg/m^3; (b) time series of $PM_{2.5}$ at representative sites (black circles on map) from July to September 2017 and 2018 from observations and simulations with ESM4_QFED (purple), with QFED_CANoff or GFED×5_CANoff (brown), with GFED×5 (red), with ESM4_ALLOff (cyan); correlations between the observed and simulated total $PM_{2.5}$, and the contribution of Canadian fires to $PM_{2.5}$ events above 35 μg/m^3 are reported.

emissions (e.g., Lin et al., 2017). With wildfire emissions turned off globally, $PM_{2.5}$ in the ESM4_AllOff experiment decreases below 10 μg/m^3 at almost all sites, indicating that anthropogenic emissions are of minor importance for summertime WUS $PM_{2.5}$ episodes (Figure 5a). During these episodes, fire emissions can explain 90% of total $PM_{2.5}$.

Hot and dry conditions in British Columbia fueled the growth of numerous wildfires during 2017 and 2018 (Figure 2). With fire emissions turned off in Canada, the GFED×5_CANoff and QFED_CANoff sensitivity experiments, relative to the respective base simulations, allow us to assess the contribution of Canadian fires. On days when observed $PM_{2.5}$ exceeds 35 μg/m^3 at sites in the Pacific Northwest, emissions from Canadian fires contribute ~50% to total $PM_{2.5}$ levels. On some days in August 2018, heavy smoke transported from British Columbia can explain almost 80% of total 60–100 μg/m^3 $PM_{2.5}$ measured at Pasayten (PASA1) and North Cascades (NOCA1), Washington. In early August 2017, smoke from British Columbia caused $PM_{2.5}$ levels across the U.S. Pacific Northwest (e.g., SNPA1 and PASA1) to exceed 35 μg/m^3.

Severe $PM_{2.5}$ episodes observed during August 2018 in Northern California and during September 2017 across the WUS are largely attributed to fires within the WUS, according to our model simulations. Specifically, the 2018 wildfire season was the deadliest and most destructive wildfire season ever recorded in California, with a total of 8,527 fires burning an area of 7.6×10^5ha, according to California Department of Forestry and Fire Protection. $PM_{2.5}$ levels of 35–85 μg/m^3 were observed at sites across Oregon and

Northern California on almost every day from late July to August 2018. This $PM_{2.5}$ episode was unprecedented in terms of duration. In early September 2017, peak $PM_{2.5}$ episodes of ~100 to 175 $\mu g/m^3$ were recorded and simulated at IMPROVE sites across the WUS (e.g., PASA1 in Washington, STAR1 in Oregon, FLAT1 in Montana, and TRIN1 in California).

4. Conclusions

Using a suite of observations and model simulations with two distinct fire emission inventories, we demonstrate the critical role of regional and distant fires in driving $PM_{2.5}$ extremes above 35 $\mu g/m^3$ measured at WUS sites. Transboundary transport of fire smoke from Canada acts as one of the key causes in addition to local fires, leading to surface $PM_{2.5}$ nonattainment in the U.S. Pacific Northwest. We reveal large uncertainties in modeling surface $PM_{2.5}$ and AOD due to uncertainties in fire emission source strength and injection height. Our analyses indicate fourfold to fivefold underestimates of organic carbon emissions from the widely used GFED. Assessing land-biosphere feedbacks on air quality in a warming climate is an area of active research (e.g., Lin et al., 2020). Evaluating the radiation and air quality impacts from increasing wildfires will rely on Earth system models with interactive fire emissions. We suggest that emission factors of aerosols used in these fire models need to be carefully evaluated and that future multimodel studies target field campaign periods to enable process-oriented analysis. Intensive field measurements of aerosols and related tracers in different ages of fire plumes for diverse fuel types may help constrain uncertainties in primary emissions and in physical and chemical processes as fire plumes age.

Data Availability Statement

Model simulations generated in this study are archived at a public data repository (at ftp://data1.gfdl.noaa.gov/users/Yuanyu.Xie/GRL2020/).

Acknowledgments
This study was supported by awards from National Oceanic and Atmospheric Administration (NOAA), U.S. Department of Commerce (NA14OAR4320106 and NA18OAR4320123). The statements, findings, conclusions, and recommendations are those of the authors and do not necessarily reflect the views of NOAA. We thank Fabien Paulot, Songmiao Fan, and Wenhao Dong for helpful discussions and comments.

References

Abatzoglou, J. T., & Williams, A. P. (2016). Impact of anthropogenic climate change on wildfire across western US forests. *Proceedings of the National Academy of Sciences*, *113*(42), 11,770–11,775. https://doi.org/10.1073/pnas.1607171113

Balch, J., Schoennagel, T., Williams, A., Abatzoglou, J., Cattau, M., Mietkiewicz, N., & St. Denis, L. (2018). Switching on the big burn of 2017. *Firehouse*, *1*(1), 17. https://doi.org/10.3390/fire1010017

Carter, T. S., Heald, C. L., Jimenez, J. L., Campuzano-Jost, P., Kondo, Y., Moteki, N., et al. (2020). How emissions uncertainty influences the distribution and radiative impacts of smoke from fires in North America. *Atmospheric Chemistry and Physics*, *20*(4), 2073–2097. https://doi.org/10.5194/acp-20-2073-2020

Cubison, M. J., Ortega, A. M., Hayes, P. L., Farmer, D. K., Day, D., Lechner, M. J., et al. (2011). Effects of aging on organic aerosol from open biomass burning smoke in aircraft and laboratory studies. *Atmospheric Chemistry and Physics*, *11*(23), 12,049–12,064. https://doi.org/10.5194/acp-11-12049-2011

Darmenov, A., & da Silva, A. M. (2015). The Quick Fire Emissions Dataset (QFED)—Documentation of Versions 2.1, 2.2 and 2.4, in: NASA technical report series on global modeling and data assimilation, NASA/TM-2015-104606, available at https://gmao.gsfc.nasa.gov/pubs/docs/Darmenov796.pdf, 2013. (Data accessed at http://ftp.as.harvard.edu/gcgrid/data/ExtData/HEMCO/QFED/v2018-07/)

Dentener, F., Kinne, S., Bond, T., Boucher, O., Cofala, J., Generoso, S., et al. (2006). Emissions of primary aerosol and precursor gases in the years 2000 and 1750 prescribed data-sets for AeroCom. *Atmospheric Chemistry and Physics*, *6*(12), 4321–4344. https://doi.org/10.5194/acp-6-4321-2006

Evans, S., Ginoux, P., Malyshev, S., & Shevliakova, E. (2016). Climate-vegetation interaction and amplification of Australian dust variability. *Geophysical Research Letters*, *43*, 11,823–11,830. https://doi.org/10.1002/2016GL071016

Garofalo, L. A., Pothier, M. A., Levin, E. J. T., Campos, T., Kreidenweis, S. M., & Farmer, D. K. (2019). Emission and evolution of submicron organic aerosol in smoke from wildfires in the western United States. *ACS Earth and Space Chemistry*, *3*(7), 1237–1247. https://doi.org/10.1021/acsearthspacechem.9b00125

Guenther, A. B., Jiang, X., Heald, C. L., Sakulyanontvittaya, T., Duhl, T., Emmons, L. K., & Wang, X. (2012). The Model of Emissions of Gases and Aerosols from Nature Version 2.1 (MEGAN2.1): An extended and updated framework for modeling biogenic emissions. *Geoscientific Model Development*, *5*(6), 1471–1492. https://doi.org/10.5194/gmd-5-1471-2012

Hallar, A. G., Molotch, N. P., Hand, J. L., Livneh, B., McCubbin, I. B., Petersen, R., et al. (2017). Impacts of increasing aridity and wildfires on aerosol loading in the intermountain western US. *Environmental Research Letters*, *12*, 014006. https://doi.org/10.1088/1748-9326/aa510a

Hand, J. L., Schichtel, B. A., Malm, W. C., & Pitchford, M. L. (2012). Particulate sulfate ion concentration and SO_2 emission trends in the United States from the early 1990s through 2010. *Atmospheric Chemistry and Physics*, *12*(21), 10,353–10,365. https://doi.org/10.5194/acp-12-10353-2012

Heald, C. L., Jacob, D. J., Turquety, S., Hudman, R. C., Weber, R. J., Sullivan, A. P., et al. (2006). Concentrations and sources of organic carbon aerosols in the free troposphere over North America. *Journal of Geophysical Research*, *111*, D23S47. https://doi.org/10.1029/2006JD007705

Hoell, A., Perlwitz, J., Dewes, C., Wolter, K., Rangwala, I., Quan, X.-W., & Eischeid, J. (2019). Anthropogenic contributions to the intensity of the 2017 United States northern Great Plains drought. *Bulletin of the American Meteorological Society*, *100*(1), S19–S24. https://doi.org/10.1175/bams-d-18-0127.1

Hoesly, R. M., Smith, S. J., Feng, L., Klimont, Z., Janssens-Maenhout, G., Pitkanen, T., et al. (2018). Historical (1750–2014) anthropogenic emissions of reactive gases and aerosols from the Community Emissions Data System (CEDS). *Geoscientific Model Development*, *11*(1), 369–408. https://doi.org/10.5194/gmd-11-369-2018

Horowitz, L. W., Naik, V., Paulot, F., Ginoux, P., Dunne, J. P., Mao, J. Q., et al. (2020). The GFDL global atmospheric chemistry-climate model AM4.1: Model description and simulation characteristics. *Journal of Advances in Modeling Earth Systems*. *in press*. https://doi.org/10.1029/2019MS002032

Jaffe, D., Hafner, W., Chand, D., Westerling, A., & Spracklen, D. (2008). Interannual variations in $PM_{2.5}$ due to wildfires in the western United States. *Environmental Science & Technology*, *42*(8), 2812–2818. https://doi.org/10.1021/es702755v

Jathar, S. H., Gordon, T. D., Hennigan, C. J., Pye, H. O., Pouliot, G., Adams, P. J., et al. (2014). Unspeciated organic emissions from combustion sources and their influence on the secondary organic aerosol budget in the United States. *Proceedings of the National Academy of Sciences*, *111*(29), 10,473–10,478. https://doi.org/10.1073/pnas.1323740111

Jolleys, M. D., Coe, H., McFiggans, G., Taylor, J. W., O'Shea, S. J., Le Breton, M., et al. (2015). Properties and evolution of biomass burning organic aerosol from Canadian boreal forest fires. *Atmospheric Chemistry and Physics*, *15*(6), 3077–3095. https://doi.org/10.5194/acp-15-3077-2015

Laing, R. J., & Jaffe, D. A. (2019). Wildfires are causing extreme PM concentrations in the western United States. *The Magazine for Environmental Managers, June*.

LeComte, D. (2019). U.S. weather highlights 2018: Another historic hurricane and wildfire season. *Weatherwise*, *72*(3), 12–23. https://doi.org/10.1080/00431672.2019.1586492

Lin, M., Fiore, A. M., Horowitz, L. W., Cooper, O. R., Naik, V., Holloway, J., et al. (2012). Transport of Asian ozone pollution into surface air over the western United States in spring. *Journal of Geophysical Research*, *117*, D00V07. https://doi.org/10.1029/2011JD016961

Lin, M., Fiore, A. M., Horowitz, L. W., Langford, A. O., Oltmans, S. J., Tarasick, D., & Rieder, H. E. (2015). Climate variability modulates western US ozone air quality in spring via deep stratospheric intrusions. *Nature Communications*, *6*(1), 7105. https://doi.org/10.1038/ncomms8105

Lin, M., Horowitz, L. W., Payton, R., Fiore, A. M., & Tonnesen, G. (2017). US surface ozone trends and extremes from 1980 to 2014: Quantifying the roles of rising Asian emissions, domestic controls, wildfires, and climate. *Atmospheric Chemistry and Physics*, *17*(4), 2943–2970. https://doi.org/10.5194/acp-17-2943-2017

Lin, M., Horowitz, L. W., Xie, Y., Paulot, F., Malyshev, S., Shevliakova, E., et al. (2020). Vegetation feedbacks during drought exacerbate ozone air pollution extremes in Europe. *Nature Climate Change*, *10*(5), 444–451. https://doi.org/10.1038/s41558-020-0743-y

Liu, X., Huey, L. G., Yokelson, R. J., Selimovic, V., Simpson, I. J., Müller, M., et al. (2017). Airborne measurements of western US wildfire emissions: Comparison with prescribed burning and air quality implications. *Journal of Geophysical Research: Atmospheres*, *122*, 6108–6129. https://doi.org/10.1002/2016JD026315

Mallia, D. V., Lin, J. C., Urbanski, S., Ehleringer, J., & Nehrkorn, T. (2015). Impacts of upwind wildfire emissions on CO, CO_2, and $PM_{2.5}$ concentrations in Salt Lake City, Utah. *Journal of Geophysical Research: Atmospheres*, *120*, 147–166. https://doi.org/10.1002/2014JD022472

May, A. A., Lee, T., McMeeking, G. R., Akagi, S., Sullivan, A. P., Urbanski, S., et al. (2015). Observations and analysis of organic aerosol evolution in some prescribed fire smoke plumes. *Atmospheric Chemistry and Physics*, *15*(11), 6323–6335. https://doi.org/10.5194/acp-15-6323-2015

McClure, C. D., & Jaffe, D. A. (2018). US particulate matter air quality improves except in wildfire-prone areas. *Proceedings of the National Academy of Sciences*, *115*(31), 7901–7906. https://doi.org/10.1073/pnas.1804353115

Mu, M., Randerson, J. T., van der Werf, G. R., Giglio, L., Kasibhatla, P., Morton, D., et al. (2011). Daily and 3-hourly variability in global fire emissions and consequences for atmospheric model predictions of carbon monoxide. *Journal of Geophysical Research*, *116*, D24303. https://doi.org/10.1029/2011JD016245

NICC. (2019). National Interagency Coordination Center (NICC) report on wildland fires and acres. https://www.nifc.gov/fireInfo/fireInfo_statistics.html*, last assessed Nov. 2019*.

O'Dell, K., Ford, B., Fischer, E. V., & Pierce, J. R. (2019). Contribution of wildland-fire smoke to US $PM_{2.5}$ and its influence on recent trends. *Environmental Science & Technology*, *53*(4), 1797–1804. https://doi.org/10.1021/acs.est.8b05430

Pan, X., Ichoku, C., Chin, M., Bian, H., Darmenov, A., Colarco, P., et al. (2020). Six global biomass burning emission datasets: Intercomparison and application in one global aerosol model. *Atmospheric Chemistry and Physics*, *20*(2), 969–994. https://doi.org/10.5194/acp-20-969-2020

Paugam, R., Wooster, M., Freitas, S., & Val Martin, M. (2016). A review of approaches to estimate wildfire plume injection height within large-scale atmospheric chemical transport models. *Atmospheric Chemistry and Physics*, *16*(2), 907–925. https://doi.org/10.5194/acp-16-907-2016

Paulot, F., Fan, S., & Horowitz, L. W. (2017). Contrasting seasonal responses of sulfate aerosols to declining SO_2 emissions in the eastern U. S.: Implications for the efficacy of SO_2 emission controls. *Geophysical Research Letters*, *44*, 455–464. https://doi.org/10.1002/2016GL070695

Petrenko, M., Kahn, R., Chin, M., & Limbacher, J. (2017). Refined use of satellite aerosol optical depth snapshots to constrain biomass burning emissions in the GOCART model. *Journal of Geophysical Research: Atmospheres*, *122*, 10,983–11,004. https://doi.org/10.1002/2017JD026693

Posner, L. N., Theodoritsi, G., Robinson, A., Yarwood, G., Koo, B., Morris, R., et al. (2019). Simulation of fresh and chemically-aged biomass burning organic aerosol. *Atmospheric Environment*, *196*, 27–37. https://doi.org/10.1016/j.atmosenv.2018.09.055

Prichard, S. J., O'Neill, S. M., Eagle, P., Andreu, A. G., Drye, B., Dubowy, J., et al. (2020). Wildland fire emission factors in North America: Synthesis of existing data, measurement needs and management applications. *International Journal of Wildland Fire*, *29*(2), 132–147. https://doi.org/10.1071/WF19066

Randerson, J. T., Chen, Y., Werf, G. R., Rogers, B. M., & Morton, D. C. (2012). Global burned area and biomass burning emissions from small fires. *Journal of Geophysical Researchs*, *117*, G04012. https://doi.org/10.1029/2012JG002128

Reddington, C. L., Spracklen, D. V., Artaxo, P., Ridley, D. A., Rizzo, L. V., & Arana, A. (2016). Analysis of particulate emissions from tropical biomass burning using a global aerosol model and long-term surface observations. *Atmospheric Chemistry and Physics*, *16*(17), 11,083–11,106. https://doi.org/10.5194/acp-16-11083-2016

Reid, C. E., Brauer, M., Johnston, F. H., Jerrett, M., Balmes, J. R., & Elliott, C. T. (2016). Critical review of health impacts of wildfire smoke exposure. *Environmental Health Perspectives*, *124*(9), 1334–1343. https://doi.org/10.1289/ehp.1409277

Remer, L. A., Kaufman, Y. J., Tanre, D., Mattoo, S., Chu, D. A., Martins, J. V., et al. (2005). The MODIS aerosol algorithm, products, and validation. *Journal of the Atmospheric Sciences*, *62*(4), 947–973. https://doi.org/10.1175/jas3385.1

Rémy, S., Veira, A., Paugam, R., Sofiev, M., Kaiser, J. W., Marenco, F., et al. (2017). Two global data sets of daily fire emission injection heights since 2003. *Atmospheric Chemistry and Physics*, *17*(4), 2921–2942. https://doi.org/10.5194/acp-17-2921-2017

Sayer, A. M., Munchak, L. A., Hsu, N. C., Levy, R. C., Bettenhausen, C., & Jeong, M. J. (2014). MODIS Collection 6 aerosol products: Comparison between Aqua's e-deep blue, dark target, and "merged" data sets, and usage recommendations. *Journal of Geophysical Research: Atmospheres*, *119*, 13,965–13,989. https://doi.org/10.1002/2014JD022453

Selimovic, V., Yokelson, R. J., McMeeking, G. R., & Coefield, S. (2019). In situ measurements of trace gases, PM, and aerosol optical properties during the 2017 NW US wildfire smoke event. *Atmospheric Chemistry and Physics*, *19*(6), 3905–3926. https://doi.org/10.5194/acp-19-3905-2019

Shrivastava, M., Cappa, C. D., Fan, J., Goldstein, A. H., Guenther, A. B., Jimenez, J. L., et al. (2017). Recent advances in understanding secondary organic aerosol: Implications for global climate forcing. *Reviews of Geophysics*, *55*, 509–559. https://doi.org/10.1002/2016rg000540

Shrivastava, M., Easter, R. C., Liu, X., Zelenyuk, A., Singh, B., Zhang, K., et al. (2015). Global transformation and fate of SOA: Implications of low-volatility SOA and gas-phase fragmentation reactions. *Journal of Geophysical Research: Atmospheres*, *120*, 4169–4195. https://doi.org/10.1002/2014JD022563

Spracklen, D. V., Logan, J. A., Mickley, L. J., Park, R. J., Yevich, R., Westerling, A. L., & Jaffe, D. A. (2007). Wildfires drive interannual variability of organic carbon aerosol in the western US in summer. *Geophysical Research Letters*, *34*, L16816. https://doi.org/10.1029/2007GL030037

The Government of British Columbia (GBC). (2019). Wildfire season summary. https://www2.gov.bc.ca/gov/content/safety/wildfire-status/about-bcws/wildfire-history/wildfire-season-summary, *last assessed Nov. 2019*.

Tosca, M. G., Randerson, J. T., & Zender, C. S. (2013). Global impact of smoke aerosols from landscape fires on climate and the Hadley circulation. *Atmospheric Chemistry and Physics*, *13*(10), 5227–5241. https://doi.org/10.5194/acp-13-5227-2013

Val Martin, M., Kahn, R., & Tosca, M. (2018). A global analysis of wildfire smoke injection heights derived from space-based multi-angle imaging. *Remote Sensing*, *10*(10), 1609. https://doi.org/10.3390/rs10101609 (Gridded data archived in https://gmd.copernicus.org/articles/11/4103/2018/gmd-11-4103-2018-supplement.zip)

van der Werf, G. R., Randerson, J. T., Giglio, L., van Leeuwen, T. T., Chen, Y., Rogers, B. M., et al. (2017). Global fire emissions estimates during 1997–2016. *Earth System Science Data*, *9*(2), 697–720. https://doi.org/10.5194/essd-9-697-2017 (Data are accessed at https://www.globalfiredata.org/)

Veefkind, J. P., Boersma, K. F., Wang, J., Kurosu, T. P., Krotkov, N., Chance, K., & Levelt, P. F. (2011). Global satellite analysis of the relation between aerosols and short-lived trace gases. *Atmospheric Chemistry and Physics*, *11*(3), 1255–1267. https://doi.org/10.5194/acp-11-1255-2011

Vicente-Serrano, S. M., Beguería, S., López-Moreno, J. I., Angulo, M., & El Kenawy, A. (2010). A new global 0.5 gridded dataset (1901–2006) of a multiscalar drought index: Comparison with current drought index datasets based on the Palmer drought severity index. *Journal of Hydrometeorology*, *11*(4), 1033–1043. https://doi.org/10.1175/2010jhm1224.1 s

Wang, H., Schubert, S. D., Koster, R. D., & Chang, Y. (2019). Attribution of the 2017 Northern High Plains drought. *Bulletin of the American Meteorological Society*, *100*(1), S25–S29. https://doi.org/10.1175/bams-d-18-0115.1

Wang, J. X. L., & Angell, J. K. (1999). Air stagnation climatology for the United States (1948–1998). *NOAA/Air Resources Laboratory ATLAS, No.1*. (data are accessed at https://www.ncdc.noaa.gov/societal-impacts/air-stagnation/)

Watson-Parris, D., Schutgens, N., Winker, D., Burton, S. P., Ferrare, R. A., & Stier, P. (2018). On the limits of CALIOP for constraining modeled free tropospheric aerosol. *Geophysical Research Letters*, *45*, 9260–9266. https://doi.org/10.1029/2018GL078195

Westerling, A. L., Hidalgo, H. G., Cayan, D. R., & Swetnam, T. W. (2006). Warming and earlier spring increase western US forest wildfire activity. *Science*, *313*(5789), 940–943. https://doi.org/10.1126/science.1128834

Winker, D. M., Tackett, J. L., Getzewich, B. J., Liu, Z., Vaughan, M. A., & Rogers, R. R. (2013). The global 3-D distribution of tropospheric aerosols as characterized by CALIOP. *Atmospheric Chemistry and Physics*, *13*(6), 3345–3361. https://doi.org/10.5194/acp-13-3345-2013

Zhao, M., Golaz, J. C., Held, I. M., Guo, H., Balaji, V., Benson, R., et al. (2018). The GFDL global atmosphere and land model AM4.0/LM4.0: 2. Model description, sensitivity studies, and tuning strategies. *Journal of Advances in Modeling Earth Systems*, *10*(3), 735–769. https://doi.org/10.1002/2017ms001209

Zhou, S., Collier, S., Jaffe, D. A., Briggs, N. L., Hee, J., Sedlacek Iii, A. J., et al. (2017). Regional influence of wildfires on aerosol chemistry in the western US and insights into atmospheric aging of biomass burning organic aerosol. *Atmospheric Chemistry and Physics*, *17*(3), 2477–2493. https://doi.org/10.5194/acp-17-2477-2017

Zhu, L., Val Martin, M., Gatti, L. V., Kahn, R., Hecobian, A., & Fischer, E. V. (2018). Development and implementation of a new biomass burning emissions injection height scheme (BBEIH v1.0) for the GEOS-Chem model (v9-01-01). *Geoscientific Model Development*, *11*(10), 4103–4116. https://doi.org/10.5194/gmd-11-4103-2018